Characterization of Limiting Factors in Laminar Flow-Based Membraneless Microfuel Cells

Electrochemical and Solid-State Letters, **8** (7) A348-A352 (2005)
1099-0062/2005/8(7)/A348/5/$7.00 © The Electrochemical Society, Inc.

Characterization of Limiting Factors in Laminar Flow-Based Membraneless Microfuel Cells

Eric R. Choban,[a,b,c] Piotr Waszczuk,[a,b,d,*] and Paul J. A. Kenis[a,b,*,z]

[a]*Department of Chemical and Biomolecular Engineering, and* [b]*The Beckman Institute, University of Illinois at Urbana-Champaign, Urbana, Illinois 61801, USA*

This paper characterizes the performance-limiting factors of a membraneless microfuel cell in which two aqueous streams flow laminarly in parallel in the absence of a physical membrane without turbulent mixing. The all-liquid configuration allows for easy external addition of a reference electrode, enabling the determination of the type of performance limiting factors such as kinetics and mass transfer limitations, including the source (anode or cathode), and the cell resistance. In addition, options to address the present dominating mass transfer limitations at the cathode are discussed.
 [DOI: 10.1149/1.1921131]

Manuscript submitted December 8, 2004; revised manuscript received February 19, 2005. Available electronically May 17, 2005.

Many efforts are underway to develop and optimize microscale fuel cells as high-energy-density power source alternatives for solid-state batteries.[1-3] One of the major challenges in these efforts is the identification of performance limiting factors. The kinetics of oxidation and reduction reactions at the electrodes, catalyst poisoning, mass transport of fuel/oxidant to the electrodes, transport phenomena across membranes (diffusion of protons and osmotic drag), and related water management (flooding and dry-out) are all possible limiting factors that need to be identified and suppressed for best possible performance. This paper reports the analysis of a microfluidic fuel cell based on laminar flow using an external reference electrode to provide insight into some of these performance-limiting phenomena, specifically mass transport and kinetic limitations.

A detailed understanding of the processes taking place at the anode and cathode, where fuel and oxidant are oxidized and reduced, respectively, is essential for fuel cell optimization efforts. The catalyst-covered anode and cathode are highly polarizable, and therefore in the presence of fuel and oxidant deviate from their respective standard electrode potentials by an overpotential as a result of slow kinetics and/or concentration effects.[4] These overpotentials result in a lower potential cell than the theoretical maximum OCP based on the standard electrode potentials. In most conventional fuel cells, the only potential that can be measured is the difference between the anode and the cathode and its change upon the application of a load. This overall cell potential does not provide thorough insight into the reasons of limiting factors at the individual electrodes. One would prefer to track the performance of the cathode and anode independently to determine the overpotentials at each electrode, and whether the fuel cell is either kinetically or mass transfer limited at the anode or cathode or both. Here we use an external reference electrode setup that allows for independent, direct evaluation of electrode performance in a laminar flow-based membraneless microfuel cell.

The use of an external reference electrode in polymer electrolyte membrane-based fuel cells (PEM-FCs) in which air or oxygen is typically delivered to the cathode in a gaseous phase has been reported.[4] Difficulties arise in these configurations due to electrode misalignment resulting in nonuniform potential distributions across the electrode surfaces and electrode polarization due to sensitivity of the reference electrode placement.[4,5] Nguyen *et al.* integrated a reference electrode by using a strip of Nafion as the electrolyte to connect the reference electrode directly with the membrane electrode assembly (MEA) thereby eliminating the need to modify the typical PEM fuel cell setup. This elegant configuration enabled a thorough analysis of electrode misalignment and flooding issues of a PEM-based fuel cell. In addition, this reference electrode configuration can in principle be integrated into any PEM-based fuel cell.

Alternatively, a gaseous dynamic hydrogen electrode (DHE) can be used as a reference in PEM-based fuel cells.[6] Fast electrode kinetics and reversibility of electro-oxidation of high-purity hydrogen gas ensure low polarization of this electrode, resulting in a well-defined reference electrode potential. By turning either the cathode or anode of a PEM-based fuel cell into a DHE, the other electrode can be characterized. Zelenay *et al.* have studied cathode performance in PEM-based cells through indirect evaluation with a DHE. Implementation of a two-electrode system within an operating fuel cell enabled the measurement of three performance curves: methanol/air, methanol/hydrogen, and a "hydrogen pump" system where hydrogen is oxidized on the anode and hydrogen is evolved on the cathode. These measurements together can then be used to calculate the cathode performance.[6] A disadvantage of the use of a DHE in this manner is that measurement of the electrode potential of both electrodes simultaneously is not feasible.

The membraneless microfuel cell analyzed here utilizes a characteristic of fluid flow at the microscale, multistream laminar flow, to keep two aqueous streams containing fuel and oxidant, respectively, separated while still in diffusional contact (Fig. 1a).[7-9] The performance of this laminar flow-based microfuel cell (LF-FC) is governed by the physicochemical phenomena of diffusion and depletion as well as the reaction kinetics at the electrodes, as we reported previously.[7-9] While in this earlier work we used polymer substrates to fabricate our LF-FCs, others have recently also reported on silicon-based LF-FCs.[10] Prior to the development of LF-FCs, Heller *et al.* reported a nonflowing microscale membraneless biofuel cell in which the anode and cathode catalysts are specific for the oxidant and fuel.[11] Such orthogonal catalysts eliminate the need for a membrane to avoid mixed electrode potentials. Unfortunately, for desired fuel/oxidant combinations such as methanol/oxygen, such orthogonal sets of catalysts of sufficient activity have not been reported to date.

In the laminar flow-based micro fuel cell (LF-FC), depletion of reactants at the electrode walls and diffusion across the mutual liquid-liquid interface are the two physicochemical phenomena that govern the conversion of chemical energy to electrical energy and mass transport phenomena. These LF-FCs avoid several of the technical issues related to the use of polymer electrolyte membranes including the occurrence of fuel crossover, electrode misalignment, and membrane dry out.[7-10] For example, fuel crossover can be avoided completely by running the LF-FC at flow rates (*i.e.*, specific residence times) in which the distance any fuel or oxidant species can diffuse into the opposing stream is less than then half the distance that separates the two electrodes. In this manner, the mixing zone can never reach the surface of the anode and cathode, thus avoiding mixed potentials due to crossover at either electrode.[7-9] Multistream laminar flow has not only been utilized successfully in these micro fuel cells, but also in similar configurations for the

* Electrochemical Society Active Member.
[c] Present address: 3M Center, St. Paul, MN, 55144-1000, USA.
[d] Present address: Guidant Corporation, St. Paul, MN 55112-5798, USA.
[z] E-mail: kenis@uiuc.edu

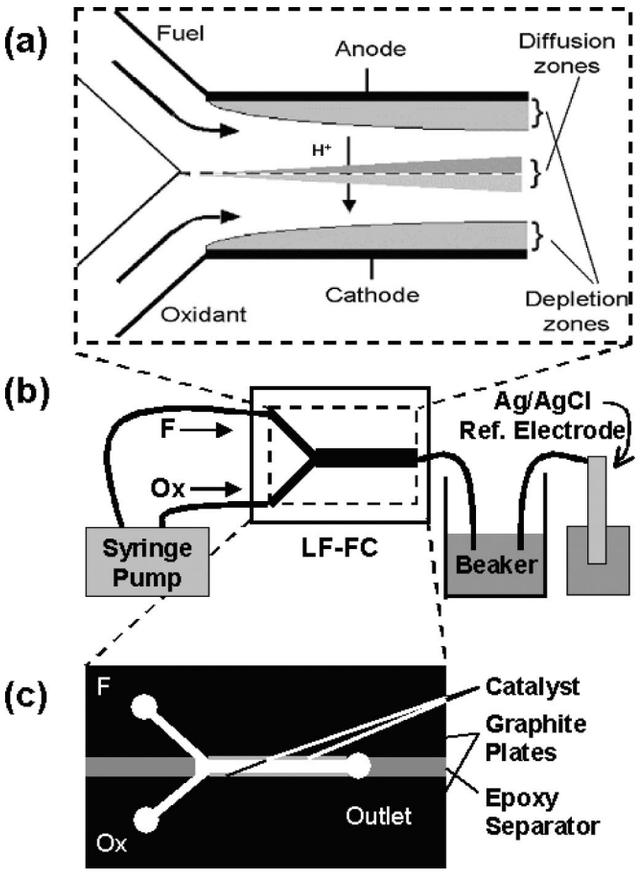

Figure 1. (a) Schematic of a membraneless fuel cell: a fuel and an oxidant stream flow laminarly in parallel between electrodes placed on opposing inside walls of a microfluidic channel. (b) LF-FC setup with an external reference electrode, which enables independent measurement of the performance of the overall fuel cell as well as of either the cathode or the anode, simultaneously. The third, not measured electrode potential is obtained by taking the difference between the two measured potentials. (c) Schematic of graphite plate configuration with epoxy separators and nanoparticle catalyst.

purpose of in-channel microfabrication,[12] microanalysis systems,[13] and redox cells.[14]

The use of a RHE or DHE as a reference electrode, commonly used in PEM-based systems as described above, is difficult when attempting to analyze individual electrode processes in an LF-FC. The limited solubility of hydrogen in the aqueous anode or cathode stream while operating the cell would cause polarization of the electrode leading to a poorly defined 'reference' potential. The lack of a membrane in an LF-FC also requires a different approach than the integrated reference electrode used by Nguyen *et al.* for PEM-based fuel cells.[4] In contrast, the all-liquid nature of the LF-FC studied here does allow for straightforward introduction of an external reference electrode, such as an off-the-shelf Ag/AgCl electrode. This paper reports the analysis of different configurations of LF-FCs through the measurement of the cell performance and assessment of the anode and cathode performance separately and simultaneously in a single experiment providing a step toward full characterization of the properties and promise of membraneless LF-FCs.

Experimental

In this study, a commercially available external Ag/AgCl reference electrode with a 3.0 M NaCl solution in its inner compartment (BASi, West Lafayette, IN) is used for individual cathode and anode analysis. This reference electrode is placed in a 1 cm diam glass compartment filled with 0.5 M sulfuric acid, which is connected to the beaker that collects the outlet stream of the LF-FC using plastic tubing (Intramedic PE205, ID = 1.57 mm) filled with 0.5 M sulfuric acid (Fig. 1b).

Graphite plates (here 1 mm thick) that serve as catalyst support, current collector, and edificial element, form the core element of the LF-FC (Fig. 1c). These plates are placed side by side to create a microfluidic channel while inlet channels for the fuel and oxidant stream are obtained by regular machining with a drill bit. Before assembly, catalyst is applied to the graphite plate's sides that line the microfluidic channel. The catalyst compositions and deposition procedures are described below. These graphite plates are aligned side by side using 0.5 or 1.0 mm epoxy separators, clamped between elastomeric gaskets and rigid support structures, such as polycarbonate, to act as a capping layer. The resulting microfluidic fuel cell thus has two parallel electrodes, separated by 0.5 or 1.0 mm, that cover the inside opposing sidewalls of a single microfluidic channel. Fuel and oxidant streams as well as the waste stream are guided into and out of the LF-FC through plastic tubing (Intramedic PE205, ID = 1.57 mm). A more detailed description of the design and fabrication of the laminar flow fuel cells used in this paper is available elsewhere.[15,16]

After passing over the anode and cathode electrodes in the LF-FC, both the fuel and oxidant streams leave the microfluidic channel jointly through a plastic tube (Intramedic PE205, ID = 1.57 mm) that empties into the same beaker as the tube connecting to the reference electrode (Fig. 1b). The distance between the external reference electrode and the fuel cell electrodes is in the order of couple of centimeters. There is no significant potential drop over this distance. Furthermore, the measured potential is not affected by the relative placement of the two plastic tubes ending in the beaker. Similarly, agitation of the solutions in the beaker had no effect on the measurements. Within the LF-FC, the entrance of the outlet tubing is centered with respect to the microfluidic channel and electrodes, and is fixed in place at least 1 mm beyond the end of the catalyst covered electrode areas. In addition, the inner diameter (1.57 mm) of this plastic outlet tube is wider than the distance (0.5 or 1.0 mm) that separates the parallel, face-to-face oriented anode and cathode electrodes in the LF-FCs studied here. As a result of these distances and relative dimensions, the potential being recorded by the external reference electrode in this work is not a local potential in the proximity of either of the electrodes as would be the case in a Luggin capillary approach, but is instead an average potential across the channel.[17] We also confirmed that upon application of a +1 V or −1 V potential difference between the anode and cathode in a LF-FC filled with electrolyte only, we measured identical but opposite potential differences between the anode and external reference electrode, and cathode and external reference electrode, respectively, showing that no significant local IR drop contributes to any potential differences measured with the external reference electrode.

Three different anode catalysts were used: (1) unsupported Pt:Ru 50:50 atomic wt % alloy nanoparticles (stock no. 41171 lot no. K28K14, Alfa Aesar); (2) a 50:50 mixture of unsupported Pt black nanoparticles and unsupported Ru nanoparticles (both Alfa Aesar); and (3) unsupported Platinum nanoparticles (Alfa Aesar). Catalyst no. 3 was also used as the cathode catalyst for all experiments. A 4.0 mg/ml catalyst suspension containing 10% by weight Nafion (Nafion stock solution: Dupont, 5 wt % solution) was created for each of the three catalyst formulations. All catalyst suspensions were applied drop-by-drop on the appropriate sides of the graphite plates by pipette and then allowed to dry using a heat lamp. Catalyst loadings varied from 2.0 to 4.0 mg/cm^2 and are in the captions of the figures.

All experiments were conducted at room temperature using 1 M methanol (99.9%, Fisher Scientific) in 18.3 Ω-cm Millipore water as the fuel (with or without 0.5 M H_2SO_4), and oxygen (99.99%, S. J. Smith Welding Supply) dissolved in 0.5 M sulfuric acid (96.5%, Fisher Scientific) in 18.3 Ω-cm Millipore water as the oxidant. Oxygen was bubbled through an aqueous solution of 0.5 M sulfuric acid for 15 min with a glass tube ending in a glass frit to aid in the

saturation of the solution. In all LF-FCs flow must be laminar to avoid turbulent mixing of the fuel and oxidant streams. Under the experimental conditions used here the Reynolds (Re) number is typically 10 or less, thus well below the laminar to turbulent flow transition region at Re~2100. Fluid flow in all of our experiments is pressure driven, leading to parabolic flow profiles, and regulated using a syringe pump (PHD 2000, Harvard Apparatus) with typical flow rates between 0.15 and 0.4 mL/min per channel. The actual flow rates, dimensions, and Reynolds numbers are given with each experiment in the captions to the figures.

Polarization curves (V *vs.* I) for fuel cell characterization were obtained using Field Point modules (National Instruments, Austin, TX) and a user interface created with Labview (National Instruments, Austin, TX). After each potential step, the current was recorded after reaching steady state, which typically took about 30 s. These transient effects are commonly observed when recording polarization curves of fuel cells. We also confirmed that these transient effects were independent of use of the external reference electrode, within the same LF-FC setup. This LF-FC setup with external reference electrode enables measurement of two parameters independently. Typically in our experiments the cathode potential and the overall cell potential were directly measured. From these two measurements the third parameter, in this work the anode potential can be calculated using $V_{cell} = V_{cathode}-V_{anode}$. Identical fuel cell polarization curves as well as identical individual anode and cathode potentials, all within the experimental error of 3%, were recorded in consecutive experiments with this setup for the same LF-FC run at the same conditions.

Results and Discussion

To further characterize the laminar flow-based membraneless fuel cell (LF-FC) we recently reported[7-9] and to further optimize its performance we included an external reference electrode. Figure 1b shows a schematic of the LF-FC setup with a Ag/AgCl external reference electrode, which enables the independent evaluation of the cell and of the anode and cathode separately and simultaneously in a single experiment. A tube filled with electrolyte, 0.5 M sulfuric acid, provides electrical contact between this external reference electrode and the LF-FC through placement in the beaker that collects the outlet stream. The overall cell potential as well as the individual potentials of the anode and cathode can be obtained by measuring independently two of the three potential differences between the three electrodes. The third potential can be calculated from the two measured potentials by addition or subtraction. For the results reported in this paper, the cathode potential and the overall cell potential are directly measured and the anode potential is calculated by subtracting the cathode potential from the overall cell potential.

Before analyzing LF-FCs, we tested whether this configuration indeed would provide a reliable means of recording potential differences between the reference electrode and the anode or cathode, respectively, in the LF-FC. The large inner diameter of the connecting tube, 1.57 mm, and the high conductivity of the 0.5 M sulfuric acid solution in the path (plastic tubing and beaker) that connects the external reference electrode to the LF-FC, ensure that no IR drop is observed between the external Ag/AgCl electrode and either the cathode or the anode, as we confirmed experimentally. While operating the fuel cell, the consumption of fuel and oxidant along the anode and cathode, respectively, leads to the formation of depletion boundary layers, which result in a non-uniform current density distribution along both electrodes. In contrast, a potential gradient along the electrodes does not occur due to the low electrical resistance of the graphite plates, less than 0.1 Ω, therefore the anode and cathode each adopt an average potential, independent of position along the length of the channel. Also, the short anode to cathode distance (0.5-1 mm) within the LF-FC compared to the diameter of 1.57 mm of the plastic tubing leading to the reference electrode and the placement of the entrance of the plastic tubing away from the anode and cathode by at least 1 mm ensure that no local IR drop within the LF-FC is measured by the reference electrode, unlike a Luggin capillary reference electrode approach.[17] This was also verified experimentally (see experimental section). Based on these considerations and experimental verifications we conclude that the configuration shown in Fig. 1b indeed provides a reliable setup to identify performance-limiting processes taking place at the individual anode and cathode electrodes in an LF-FC.

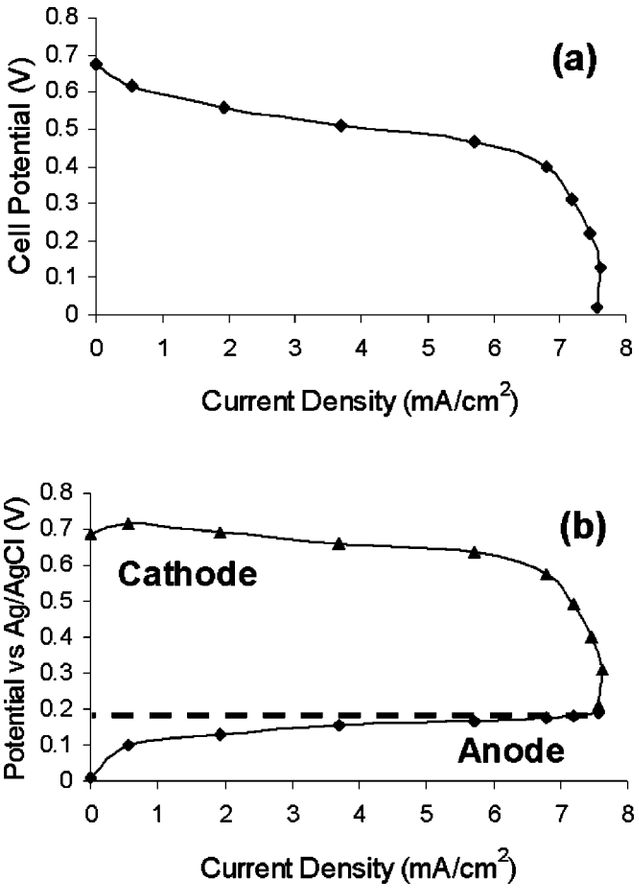

Figure 2. Reference electrode experiment to isolate cathode and anode performance in an LF-FC. Polarization curves for (a) the overall cell performance; and (b) the individual anode and cathode. Fuel: 1.0 M methanol in 0.5 M H_2SO_4. Oxidant: oxygen-saturated 0.5 M H_2SO_4. Anode and cathode catalysts are Pt:Ru 50:50 alloy unsupported nanoparticles and Pt black unsupported nanoparticles, respectively, at a loading of 2.0 mg/cm^2. Flow rate: 0.3 ml/min per inlet channel. Channel length: 2.9 cm, width: 1.0 mm, height: 1 mm. Re = 6.7. Experimental error ±3%.

A number of different LF-FCs were analyzed with the external reference electrode configuration. Figure 2a shows polarization curves of the overall performance of a LF-FC run with 1.0 M methanol in 0.5 M sulfuric acid and oxygen-saturated 0.5 M sulfuric acid as the fuel and oxidant stream, respectively. The anode catalyst is 4.0 mg/cm^2 Pt:Ru alloy nanoparticles while the cathode catalyst is 4.0 mg/cm^2 Pt black nanoparticles. The sharp decline of the potential at current densities >7 mA/cm^2 indicates that the process is mass transfer limited at higher current densities. In our earlier work, we observed improved performance as a function of increasing flow rate, already providing evidence of a mass-transfer limitation.[7] No conclusion, however, can be drawn from the overall cell potential curve of Fig. 2a whether this mass transfer limitation occurs at the anode or at the cathode. Use of an external Ag/AgCl reference electrode, connected to the LF-FC as shown in Fig. 1, enables acquisition of the individual contributions of the anode and cathode processes, Fig. 2b, to the overall cell performance, Fig. 2a. The shape and respective potential drops of these individual anode and cathode

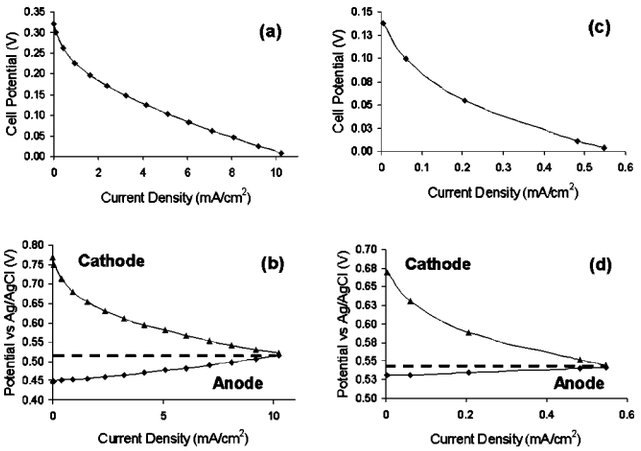

Figure 3. Polarization curves of overall cell performance, (a) and (c), and individual cathode and anode performances measured separately versus the external Ag/AgCl reference electrode, (b) and (d). Fuel: 1.0 M Methanol. Oxidant: oxygen-saturated 0.5 M H_2SO_4. Anode catalyst is Pt:Ru mixture 50:50 unsupported nanoparticles for (a) and (b), and Pt unsupported nanoparticles for (c) and (d). The cathode catalyst is Pt unsupported nanoparticles for all experiments. All catalysts are applied at a loading of 4.0 mg/cm^2. Flow rate: 0.1 ml/min per inlet channel. Channel length: 2.9 cm, width: 0.50 mm, height: 1 mm. Re = 3.3. Experimental error ±3%.

polarization curves show that mass transfer at the cathode limits cell performance at high current densities for this particular LF-FC operated under these conditions. The oxidant-containing stream is depleted first, as expected, due to the low solubility of oxygen in the water-based electrolyte, about 2-4 mM at room temperature and standard pressure.[18]

Whether or not the relative potentials measured between the anode (or cathode) and the reference electrode represent potentials of the individual electrodes alone depends in part on the composition/conductivity of the liquid streams that separate the anode and the cathode. In the LF-FC experiments shown in Fig. 2, both the cathode and anode streams are composed of a conductive 0.5 M sulfuric acid solution with the LF-FC generating maximum current densities on the order of 10 mA/cm^2. The high electrolyte concentration leads to a very low internal cell resistance, and, as a result, the potential drop or loss across the electrolyte between the anode and cathode is negligible. Potential differences measured between the anode (or cathode) and the Ag/AgCl reference electrode can thus be attributed exclusively to the anode (or cathode). Figure 2b shows that a cathode potential of ~0.7 V (*vs.* Ag/AgCl) is obtained in this LF-FC for oxygen reduction. After correction for the 0.22 V potential difference between a Ag/AgCl reference electrode and a RHE,[17] the cathode potential of 0.7 V *vs.* Ag/AgCl measured here is in agreement with, for example, the oxygen reduction potential of 0.9 V *vs.* RHE reported by Zelenay *et al.*[6]

In previous work, we used electrodeposited Pt-black electrodes,[7] whereas we use nanoparticle-based catalysts here. The higher active catalytic surface area of these nanoparticles (surface roughness factor of ~500 as opposed to ~80 for electrodeposited platinum) as well as the use of bimetallic catalysts to address CO poisoning of the anode, resulted in an increase of the maximum current density from 0.8 mA/cm^2, our earlier work using formic acid as the fuel,[7] to approximately 8 or 10 mA/cm^2 (Fig. 2 and 3, respectively). The maximum power density for this LF-FC is 2.8 mW/cm^2. This performance also exceeds the maximum current and power densities of silicon-based LF-FCs run on formic acid with a Bi-based catalyst as reported by Cohen *et al.*[10]

The LF-FC configuration studied above (Fig. 2), which had the best presently known catalysts for methanol oxidation and oxygen reduction, respectively, was determined to be cathode-limited by mass transfer. Next, we decided to use the LF-FC with external reference electrode configuration to show that also LF-FCs with kinetic limitations can be characterized. We constructed LF-FCs that were intentionally anode-limited for methanol oxidation with the integration of non-ideal catalysts of 4.0 mg/cm^2 50:50 Pt:Ru mixture of nanoparticles (Fig. 3a and b) and 4.0 mg/cm^2 Pt black nanoparticles (Fig. 3c and d). These anode catalysts both are known to suffer from CO poisoning during the electro-oxidation of methanol,[19] and thus are good candidates to purposely create kinetically limited LF-FCs. These LF-FCs all had 4.0 mg/cm^2 Pt black nanoparticles as the cathode catalyst for oxygen reduction and they were operated with 1.0 M methanol as the fuel stream and oxygen-saturated 0.5 M sulfuric acid as the oxidant stream. Supporting electrolyte was left out of the fuel stream to demonstrate that the use of the reference electrode clearly allows for characterization of the response of an individual electrode to a change of experimental conditions such as the presence or absence of the electrolyte.

The polarization curve of a cell with 50:50 Pt and Ru mixture of nanoparticles as the anode catalyst is shown in Fig. 3a, while the individual anode and cathode polarization contributions to the overall cell performance are shown in Fig. 3b. Figure 3b indicates that this LF-FC, as intended, is anode limited: the higher anode potential results in lower open cell potential as will be further discussed below. The difference in the shape of the overall cell polarization curve from typical fuel cell performance curves (see for example Fig. 2a) is caused by the lack of electrolyte in the anode stream, leading to a higher cell resistance. Thus the performance curve looks more like the I-V curve of a resistor, a straight line.

Figures 3c and d show, respectively, the overall cell polarization curve and the corresponding individual anode and cathode polarization curves of an identical LF-FC run under identical conditions but with 4.0 mg/cm^2 Pt black nanoparticles as the anode catalyst. The performance of the LF-FC of Fig. 3a and b discussed above is clearly better; more than 10 times higher current densities are measured at similar cell potentials than of the LF-FC of Fig. 3c and d. This difference in cell performance clearly indicates an even more severe reaction kinetics limitation at the anode of the LF-FC experiment shown in Fig. 3c and d.

As expected, a Pt nanoparticle catalyst based-anode suffers even more from CO poisoning than the mixture of Pt and Ru nanoparticles (Fig. 3a and b). The decrease in performance can be seen by comparing the onset of the anode curves (at zero current) in Fig. 3d and b: under open-circuit conditions the electro-oxidation potential of methanol is approximately 0.1 V higher (*i.e.*, less negative) using Pt nanoparticles (Fig. 3d) as opposed to a mixture of Pt and Ru nanoparticles (Fig. 3b) as the catalyst, resulting in a reduction of the open cell potential for the former.

For the LF-FC experiments shown in Fig. 3, in which the cathode does contain electrolyte, 0.5 M H_2SO_4, but the anode stream does purposely not contain electrolyte, the relative potentials measured between the anode (or cathode) and the reference electrode do not represent potentials of the individual electrodes alone. The IR drop across the cell from the cathode to the anode is highly nonlinear. Any potential measured with the reference electrode will include contributions from the individual electrode potential (anode or cathode) and from potential losses in the electrolyte. This situation is not unique to LF-FCs because it is also encountered in thin gap fuel cells.[4,5] In the LF-FC system described here, positive or negative effects of any change in the cell dimensions, fuel/oxidant/catalyst combinations used, operating conditions, etc. can be analyzed qualitatively and quantitatively among different LF-FC experiments only if the electrolyte composition of the two streams are identical. The performance curves of the mass transfer limited LF-FC of Fig. 2 and the purposely reaction kinetics-limited LF-FCs of Fig. 3 differ in shape for two reasons: First, the fuel stream (anode) in the experiment of Fig. 2 contains supporting electrolyte, 0.5 M sulfuric acid as opposed to no electrolyte in the fuel stream of the experiment in Fig. 3, and thus improves conductivity of the cell leading to a cell polar-

ization curve that is characteristic in shape for a fuel cell (Fig. 2) rather than a resistor (Fig. 3). Second, the OCPs for the LF-FCs of Fig. 2 and 3 differ substantially, 0.7 V *vs.* 0.3 V or less, respectively. With the cathode catalyst and oxidant stream composition being the same for all experiments reported in this paper, the majority of the differences in cell performance can be attributed to differences in anode performance. While in Fig. 2 the anode curve starts at about 0.0 V *vs.* Ag/AgCl, the anode curves in Fig. 3 start at about 0.5 V *vs.* Ag/AgCl. This difference in anode potentials at open circuit is a result of the difference in conductivity and acidity of the respective fuel streams and especially of the difference in anode catalyst. Pt:Ru alloy particles were used as the anode catalyst in the fuel cells studied in Fig. 2, whereas a mixture of Ru and Pt nanoparticles were used as the anode catalyst for the purposely anode-limited LF-FC of Fig. 3a and b. For efficient methanol electro-oxidation both Ru and Pt sites are necessary in close proximity to oxidize the absorbed carbon monoxide poisoning species into carbon dioxide. In the mixture of Pt and Ru nanoparticles, the nanoparticles are randomly dispersed and good electro-oxidation sites only exist when Pt and Ru nanoparticles are in contact with each other. In the case of the Pt:Ru alloy nanoparticle catalyst, suitable electro-oxidation sites for methanol are present all over the surface of all nanoparticles.

Conclusion

The LF-FC configuration with external Ag/AgCl reference electrode used here allowed for unambiguous identification of performance-limiting factors of membraneless LF-FCs. Characterization of the overall LF-FC performance and of the individual electrodes can be performed under load conditions without the results being confused with other issues that are typical to Nafion-based systems such as electrode placement, misalignment of electrodes, and water management. The individual contributions of the anode and cathode potentials to the overall cell potential can be obtained simultaneously for an LF-FC in a single experiment and from these data, the nature (mass transfer or reaction kinetics limitation) and origin (anode or cathode) of specific performance-limiting factors of LF-FCs can be determined. Moreover, in experiments in which both the anode stream and cathode stream contain electrolyte and thus are highly conductive (*i.e.*, low cell resistance, negligible IR drop in solutions), relevant anode and cathode potentials (*vs.* Ag/AgCl) can be obtained.

This LF-FC configuration with an external reference electrode allowed for detailed analysis of the LF-FC presently providing best performance, using methanol as the fuel and Pt and Pt/Ru alloy nanoparticles as the cathode and anode catalysts, respectively. This analysis confirmed our earlier hypothesis[7-9] that these fuel cells become limited at the cathode beyond certain current densities, here >7 mA/cm^2, due to the low solubility of oxygen in aqueous media and the resulting mass transfer limitations in the oxygen depleted boundary layer. Still, this LF-FC comprised of graphite plates as catalyst support and current collector outperforms our previous LF-FCs[7-9] as well as those recently reported by others.[10]

In this paper we also showed that the LF-FC configuration with external reference electrode could correctly identify performance-limiting factors due to poor reaction kinetics. LF-FCs purposely provided with anode catalysts that are known to be prone to CO poisoning, Pt nanoparticles, or a mixture of Pt and Ru nanoparticle, indeed exhibited performance curves dominated by kinetic limitations at the anode, as expected. Much lower open-circuit potentials and current densities were measured for these LF-FCs. While the nature of the performance-limiting factor of 'poor reaction kinetics' can be identified, kinetic parameters cannot easily be deduced from these measurements due to the nonuniform current density distribution along the electrodes.

This work represents a step toward a more complete characterization of the properties of membraneless LF-FCs. Guided by a better understanding of the performance limiting factors in LF-FCs, multiple changes in the design and operation conditions of these conceptually novel micro fuel cells can be considered, especially to overcome the herein identified mass transfer limitations at the cathode imposed by the low oxygen solubility in the liquid stream. One could decide to supply the cathode with a higher flux of oxygen through a PDMS membrane, like Nuzzo *et al.* in their recently published micro fuel cell work.[20] Alternatively, we have been able to increase the oxygen storage capacity of the aqueous oxidant stream by using perfluoro-carbon emulsions, which are used for that purpose in a wide range of medical applications.[21] Both these options, however, seem to be limited to an increase of the oxygen concentration by a factor of five. Another option that we are presently exploring is the repeated replenishment (or repeated removal) of the depleted boundary layer by having multiple inlets (or outlets) along the length of the cathode. We will report shortly on our findings of these studies. Also, we are presently exploring changes to the design to enhance the fuel utilization, presently less than 15%, either by changes to the individual LF-FC design or by system level solution such as recirculating streams.

Acknowledgments

The authors acknowledge generous support by the University of Illinois, the Beckman Institute, and INI Power Systems which provided a subcontract of an Army Research Office Phase I STTR grant (DAAD19-03-C-0094) for this project. Also, we acknowledge Professor Andrzej Wieckowski, Seong Kee Yoon, Jacob Spendelow, and Dr. Lajos Gancs for stimulating discussions.

The University of Illinois at Urbana-Champaign assisted in meeting the publication costs of this article.

References

1. A. S. Patil and R. Jacobs, *IEEE Aerosp. Electron. Syst. Mag.* **3**, 35 (2000).
2. C. W. Moore and P. A. Kohl, in *Microfabricated Systems and MEMS VI*, P. Hesketh, S. S. Ang, J. L. Davidson, H. G. Hughes, and D. Misra, Editors, PV 2002-6, p. 183, The Electrochemical Society Proceedings Series, Pennington, NJ (2002).
3. W. Y. Sim, G. Y. Kim, and S. S. Yang, in *MEMS*, IEEE, p. 341 (2001).
4. W. He and T. V. Nguyen, *J. Electrochem. Soc.*, **151**, A185 (2004).
5. Z. Liu, J. S. Wainright, W. Huang, and R. F. Savinell, *Electrochim. Acta*, **49**, 923 (2004).
6. S. C. Thomas, X. Ren, S. Gottesfeld, and P. Zelenay, *Electrochim. Acta*, **47**, 3741 (2002).
7. E. R. Choban, L. J. Markoski, A. Wieckowski, and P. J. A. Kenis, *J. Power Sources*, **128**, 54 (2004).
8. E. R. Choban, P. Waszczuk, L. J. Markoski, A. Wieckowski, and P. J. A. Kenis, in *Proceedings of the International Conference on Fuel Cell Science Engineering and Technology*, p. 261 (2003).
9. E. R. Choban, L. J. Markoski, J. Stoltzfus, J. S. Moore, and P. J. A. Kenis, in *Proceedings of the 40th Power Sources Conference*, Cherry Hill, NJ, IEEE, p. 317 (2002).
10. J. L. Cohen, D. A. Westly, A. Pechenik, and H. D. Abruña, *J. Power Sources*, In press.
11. N. Mano and A. Heller, *J. Electrochem. Soc.*, **150**, A1136 (2003).
12. P. J. A. Kenis, R. F. Ismagilov, and G. M. Whitesides, *Science*, **285**, 83 (1999).
13. K. Macounova, C. R. Cabrera, and P. Yager, *Anal. Chem.*, **73**, 1627 (2001).
14. R. Ferrigno, A. D. Stroock, T. D. Clark, M. Mayer, and G. M. Whitesides, *J. Am. Chem. Soc.*, **124**, 12930 (2002).
15. E. R. Choban, P. Waszczuk, A. Wieckowski, and P. J. A. Kenis, *In preparation*.
16. L. J. Markoski, P. J. A. Kenis, and E. R. Choban, U.S. Pat. Appl. Publ. 20040072047 (2004).
17. G. Prentice, *Electrochemical Engineering Principles*, Prentice Hall, Upper Saddle River, NJ (1991).
18. *CRC Handbook of Chemistry and Physics*, 70th Edition, R. C. Weast, D. R. Lide, M. J. Astle, and W. H. Beyer, Editors, p. D-274, CRC Press, Boca Raton, FL (1989).
19. W. Chrzanowski and A. Wieckowski, *Langmuir*, **14**, 1967 (1998).
20. S. Mitrovski, L. Elliott, and R. Nuzzo, *Langmuir*, **20**, 6974 (2004).
21. E. Kissa, *Fluorinated Surfactants: Synthesis, Properties, Applications*, Marcel Dekker Publisher, New York (1993).